2026 IEEE/SICE International Symposium on System Integration (SII)
January 11-14, 2026. Cancún, México

Vibrotactile Feedback Enhancement for Polishing Tasks: A Perceptual Study of Signal Deformation Strategies

Amane Tamada[1], Shogo Sakairi, Natsuki Hayami, Naruhiro Mega, Rie Nishihama, Takako Yoshida, Taro Nakamura, *Member, IEEE,* and Manabu Okui, *Member, IEEE*

***Abstract*— In the teleoperation of skilled manual tasks such as precision polishing, haptic feedback with a high degree of fidelity is considered essential. However, matching the dynamic characteristics of the leader and follower systems is challenging, often degrading feedback quality. This degradation can impair demonstration data and reduce learning performance for both machine learning systems and human users. Conventional solutions have relied on complex hardware or control schemes, increasing cost and limiting applicability. Several studies have explored improving haptic perceptual quality via minimal-cost vibrotactile signal processing, deforming or exaggerating the original haptic signal. To examine the effects of different processing strategies, we compared four vibrotactile deformation methods: perceptual low-pass filtering, frequency-bin amplitude change emphasis, envelope-based nonlinear gain, and task-specific band-pass filtering emphasizing vibration features identified from real polishing data. Pre-recorded vibrations were processed offline and presented to participants using a custom mock polisher with two voice-coil actuators. A perceptual evaluation revealed no significant differences in switch response behavior to vibration changes, indicating contact and pressing of the metal surface. In contrast, the task-specific band-pass filtering condition yielded significantly higher clarity, naturalness, and confidence scores than the others. The main contributions of this work are the development of a low-cost, medium-fidelity metal mock polisher and a task-specific vibration frequency deformation strategy for polishing, which can improve the perceived clarity of pressing sensations compared to both the strategies drawn from prior work and all other strategies tested here.**

I. Introduction

High-quality demonstration data are usually believed to be indispensable for automating complex manual skills. Such data are often acquired via bilateral control systems that transmit haptic sensations from remote tools to an operator [1], and subsequently utilized for imitation learning [2]. Haptic feedback tends to be believed to play a critical role in enabling realistic and intuitive interaction with remote or virtual environments [3]. In teleoperation, fidelity of haptic feedback often strongly influences the end-user's performance in tasks such as complex machining [4] and delicate surgical operations [5].

However, maintaining high fidelity during delicate operations used to be technically challenging. For example, dynamics mismatches between leader and follower systems inherently degrade both force and vibrotactile feedback quality. In general, fidelity and transparency of feedback are in a trade-off relationship with stability, and lead to the difficulty in improving quality without compromising control stability [6]. This degradation can diminish the richness and accuracy of demonstration data, reduce learning performance, and hinder the automation of complex skills.

Approaches for this problem have focused on improving haptic models, developing complex hardware, or optimizing control strategies. For example, Kuchenbecker *et al.* [7] modeled frequency responses based on recorded acceleration, Okamura *et al.* [8] determined optimal parameters for vibration simulation through psychophysical experiments, Wang *et al.* [9] attempted to improve haptic fidelity by adaptively updating controller parameters according to online impedance estimation, Ji *et al.* [10] recognized contact states via machine learning to achieve discriminable physical interactions, and Yao *et al.* [11] and MacLachlan *et al.* [12] improved feedback intensity and stability through hardware upgrades. While these methods offer solutions, they often require substantial redesign, increased cost, or have limited applicability.

In response, we employ an alternative approach that enhances the human perceptual quality of vibrotactile feedback by processing the signal based on task-specific vibration characteristics, human tactile characteristics, and the actuator's frequency response characteristics. Since this approach focuses primarily on perceptual signal modulation, as long as the processing is fast, perceptual quality can be improved without directly affecting the physical stability of the control loop. Human sensitivity to vibration, such as the high-frequency sensitivity of Pacinian corpuscles, has been well studied [13], [14], forming the basis for haptic rendering. Prior work has examined the envelope effect in collision vibration perception [15], [16], perceptual filtering for signal compression and clarification [17], and frequency-selective deformation methods [18]. However, there is a lack of systematic comparisons evaluating the impact of multiple signal deformation strategies on the perceptual quality of skilled manual work.

We hypothesize that selectively processing perceptually important elements can improve haptic quality even when using standard, readily available actuators. In this study, we focus on decorative polishing and compare several strategies, including those proposed in prior studies. Using acceleration data from a professional polisher, we apply offline signal compensation and present the vibrations through a mock

*This work was supported in part by the New Energy and Industrial Technology Development Organization (NEDO) under Project No. 20250000000188.

[1]A. Tamada is with the Department of Precision Mechanics, Faculty of Science and Engineering, Chuo University, Tokyo, Japan a21.jny3@g.chuo-u.ac.jp

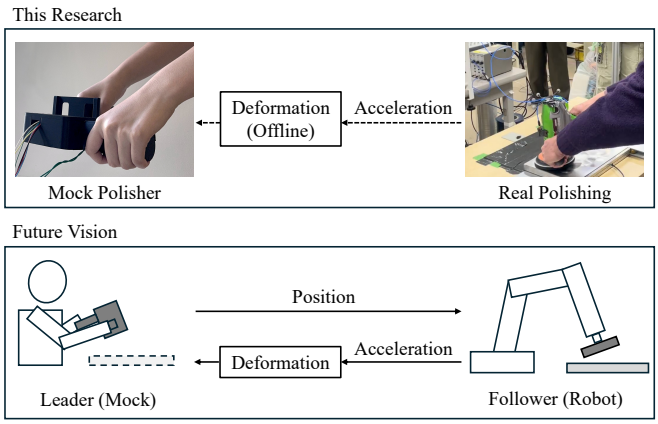

Fig. 1: Overview of the study. At this stage, reported here, the polishing vibration data were processed offline and presented via a mock polisher. Our future work can involve real-time integration into a bilateral control system, enabling task-specific vibrotactile enhancement without compromising stability.

polisher, as illustrated in Fig. 1.

The contributions of this work are as follows:

1) Development of a low-cost, medium-fidelity mock polisher equipped with voice-coil actuators for vibrotactile feedback presentation.
2) A comparative evaluation of multiple signal deformation strategies optimized for skilled manual polishing task.
3) Demonstration that band-pass filtering tuned to a frequency band selected based on polishing task characteristics can effectively improve the perceived clarity of pressing sensations.

II. Data Acquisition

This section describes the acquisition of vibration and force data from a professional polisher, which served as the basis for designing and evaluating the proposed signal deformation strategies. The polisher was an active decorative polishing craftsman, age 56, with 27 years of professional experience, who participated as a research collaborator and contributed the data on a voluntary, unpaid basis. The goal was to capture representative polishing dynamics that contain both steady-state and transient components, enabling a meaningful assessment of each processing method. As an initial step, we focused on an edge-pressing action that combines continuous vibration with abrupt changes, making it easier to identify and evaluate perceptually relevant signal features.

The overall measurement system is shown in Fig. 2. The setup consisted of two subsystems: acceleration measurement and force measurement. For acceleration, a three-axis accelerometer (NP-3572, TEAC) was affixed to the housing of the polisher using adhesive tape. The accelerometer output was amplified and digitized at a 10 kHz sampling rate using a dSPACE MicroLabBox, and stored on a PC. For force, a force plate was installed beneath the workpiece to detect the presence of pressing and to measure changes in contact force.

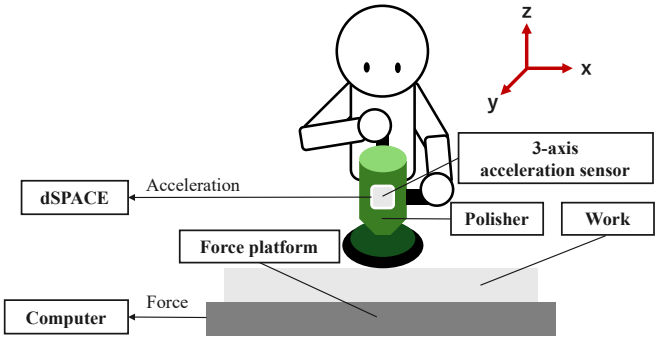

Fig. 2: Experimental setup for polishing data acquisition. A three-axis accelerometer was affixed to the polisher with tape, and a force plate was placed beneath the workpiece to record pressing force. Acceleration signals were amplified and digitized by a dSPACE MicroLabBox, while force plate data were recorded directly to a PC.

The force signals were digitized at 1 kHz and recorded on a separate PC. Since the two systems were not hardware-synchronized, their timelines were aligned manually by visual inspection of corresponding transient events in the acceleration and force signals. The alignment accuracy was within tens of milliseconds, which is sufficient given the temporal resolution required for the analyses in this study.

Measurements were conducted in a quiet indoor laboratory environment to minimize acoustic and vibrational disturbances. The workpiece was an untreated metal sample prior to surface finishing. The polisher's no-load rotational speed was 18,000 rpm; under load, the speed decreased slightly due to contact forces. The professional polisher executed the decorative polishing patterns commonly used in practice, such as straight-line and random scale patterns. In this experiment, we selected the random scale pattern, which is produced by pressing the edge of the polisher against the workpiece while moving it in a pseudo-random trajectory. This action was repeated three times, and acceleration and force data were collected simultaneously in each trial.

The representative data in Fig. 3 include forces and accelerations along the x-, y-, and z-axes, and spectrograms for each acceleration. Periods where the z-axis force was negative correspond to intervals when the polisher was pressed against the workpiece. The raw acceleration data reveal amplitude modulation depending on pressing, with a pronounced $\sim$300 Hz component along the y-axis corresponding to the polisher's rotation. This frequency decreases when pressed, and a low-frequency component around 50 Hz appears exclusively during contact. These observations directly informed the selection of frequency ranges and processing methods described in Section III.

III. Signal Deformation Strategy

This section describes the signal deformation strategies applied to the recorded vibration signals. To provide an overview of how these strategies alter the vibration characteristics, Fig. 4 presents difference spectrograms relative to the unprocessed condition. These plots highlight the frequency

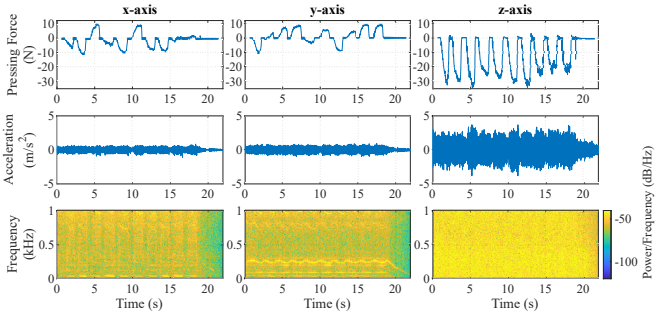

Fig. 3: Example of recorded data during a random scale decorative polishing pattern performed by a professional craftsman. From top to bottom: forces and accelerations along x-, y-, and z-axis, and spectrograms corresponding to the accelerations. Pressing periods (negative z-axis force) show increased acceleration amplitude, a strong 300 Hz rotation component along the y-axis, and a contact-induced low-frequency vibration around 50 Hz. Color scale indicates power spectral density in dB/Hz.

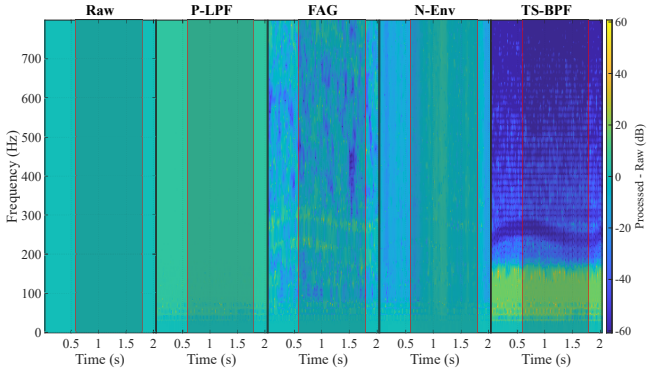

Fig. 4: Difference spectrograms showing the change in spectral power relative to the Raw condition for each signal deformation strategy. Positive values indicate increased power compared to Raw, and negative values indicate reduced power. Red vertical lines and light gray shaded regions denote the start and end of pressing intervals. Frequency range is limited to 0–800 Hz for clarity, with a common color scale applied across all conditions.

– time regions where each method increases or decreases signal energy, with red lines marking the start and end of pressing intervals.

Based on the vibration characteristics observed in Section II, we designed and evaluated four signal deformation strategies aimed at enhancing perceptually important features in polishing tasks. Here, signal deformation refers to feature-emphasizing processing applied to the measured acceleration signals prior to presentation. All strategies shared a common preprocessing pipeline: (1) use of the y-axis acceleration, which exhibited the most prominent vibration characteristics; (2) frame-by-frame processing to allow for potential real-time implementation; and (3) normalization of each processed frame so that its maximum value matched the actuator's input limit, thereby maximizing output without clipping.

A. Perceptual Low-Pass Filtering

Human vibrotactile sensitivity is reported to peak around 250 Hz and declines markedly above 500–1,000 Hz [13]. Following prior haptic rendering studies [19], [20], we applied a low-pass filter with a 1 kHz cutoff to the raw data. This condition served as a perceptually motivated baseline, preserving frequency components most relevant to human perception while removing high-frequency content that is poorly perceived and may introduce actuator inefficiency.

B. Frequency-Bin Amplitude Change Emphasis

Section II showed that frequency components corresponding to polisher rotation shifted downward under load. We hypothesized that emphasizing frequencies exhibiting large amplitude changes between successive frames would make pressing timing and force more noticeable. For each frequency bin k, the gain was computed as:

$$G_n(k) = |X_n(k)| - |X_{n-1}(k)|\,, \tag{1}$$

where $|X_n(k)|$ is the magnitude of bin k in frame n and $|X_{n-1}(k)|$ is that of the previous frame. This inter-frame difference emphasizes only frequency components that change over time. Negative gains were retained to preserve directional change information; overall gain was normalized to the actuator's range. We expected this to highlight transient frequency shifts associated with pressing.

C. Envelope-Based Nonlinear Gain

The measured signals exhibited amplitude modulation related to pressing force. To enhance this perception, we computed the temporal envelope using the Hilbert transform, obtaining the analytic signal $s_a(t) = s(t) + j\hat{s}(t)$, where $s(t)$ denotes the pre-processed time-domain signal before the enhancement, $\hat{s}(t)$ is the Hilbert transform of $s(t)$, and $E(t) = |s_a(t)|$ is the envelope. The enhanced signal was then given by:

$$E_{\text{enhanced}}[n] = s[n] \cdot |\Delta E[n]|^k\,, \tag{2}$$

where $\Delta E[n]$ is the temporal change in the envelope and k controls emphasis strength. We set $k = 5$ based on pilot tests as the maximum emphasis achievable without attenuating weaker components below the actuator's minimum effective output after normalization. This method primarily enhances transient changes such as contact onset and offset, with minimal effect on steady-state vibration perception.

D. Task-Specific Band-Pass Filtering

Spectrogram analysis in Section II revealed a narrow-band vibration around 5–150 Hz that appeared only during pressing. We designed a band-pass filter with this pass-band, chosen to include the characteristic contact-induced component while remaining within the actuator's effective frequency range. Similar task-specific frequency selection approaches have been reported [18], but here the passband was explicitly determined from our polishing data and actuator characteristics. We expected this targeted filtering

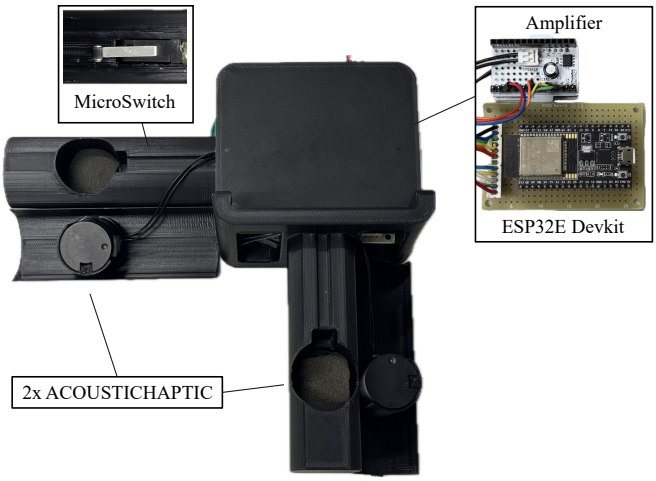

Fig. 5: Schematic of the developed mock polisher. Two voice-coil actuators (ACOUSTICHAPTIC) are embedded in the handles, mechanically isolated from the main body via sponge mounts. The left handle includes a switch for experimental input.

to selectively enhance the sensation of pressing without introducing unrelated spectral content.

IV. Experimental Setup

This section describes the hardware implementation of the mock polisher and the overall experimental system used for vibration presentation and evaluation.

A. Mock Polisher Design

The mock polisher (Fig. 5) was fabricated via fused-filament 3D printing using polylactic acid (PLA) material. The assembled device, including cabling, weighed 375 g and measured 191 mm $\times$ 196 mm $\times$ 80 mm. The handle geometry was designed to closely resemble that of a commercial rotary polisher to facilitate natural grip and operation.

Each handle housed a vertically oriented voice-coil actuator (ACOUSTICHAPTIC), mechanically isolated from the main body via sponge coupling to reduce vibration loss. The actuators were selected to reproduce a wide range of vibration frequencies present in polishing tasks, with a peak acceleration output at approximately 65 Hz, enabling presentation of both low-frequency vibration components associated with pressing contact and higher-frequency texture components. This selection balanced frequency bandwidth and output force while maintaining low mass for handheld operation.

The left handle was equipped with a lever-actuated snap-action limit switch, positioned for easy access, to record participant responses during evaluation trials.

B. System Configuration

The experimental system (Fig. 6) integrated the mock polisher with an ESP32 DevKit-C microcontroller and a dSPACE real-time control system. A PC running a graphical user interface (GUI) allowed the experimenter to select the vibration condition in real time. The vibration signals were

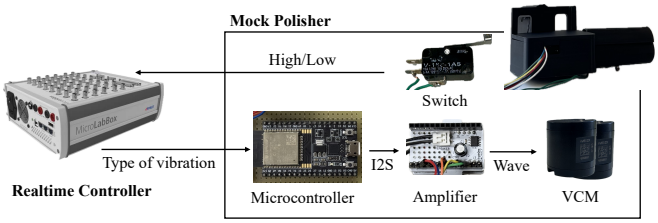

Fig. 6: System configuration. The mock polisher communicates with the dSPACE real-time control system via ESP32, which in turn interfaces with a PC for stimulus control. Switch presses are logged by the dSPACE system.

preloaded in the microcontroller's memory, and the dSPACE system controlled which signal was played back via digital I/O. The selected signal was converted to an analog drive signal for the actuators and amplified before presentation. Switch states from the left handle were recorded by the dSPACE system and logged on the PC for subsequent analysis.

V. Perceptual Evaluation

This section describes the experimental procedure for evaluating the perceptual effects of the four signal deformation strategies.

A. Stimulus Conditions

Five stimulus conditions were tested:

1) **Raw**: Unprocessed vibration data recorded from a professional polisher.
2) **P-LPF** (Perceptual Low-Pass Filtering): Raw data low-pass filtered at 1 kHz.
3) **FAG** (Frequency-Bin Amplitude Gain): P-LPF data with gain applied to frequency bins according to inter-frame amplitude change [Eq. (1)].
4) **N-Env** (Envelope-Based Nonlinear Gain): P-LPF data with gain applied according to the Hilbert envelope [Eq. (2)], with exponent $k = 5$ chosen experimentally to maximize emphasis while keeping weaker components above the actuator's minimum effective output after normalization.
5) **TS-BPF** (Task-Specific Band-Pass Filtering): P-LPF data filtered with a passband of 5–150 Hz, selected based on the characteristic frequency range of pressing contact in polishing.

Two different datasets were prepared for each condition, each containing one press/release action, to introduce variation in pressing timing and vibration characteristics. This resulted in 10 distinct stimuli.

B. Participants

Ten healthy university students (7 male, 3 female, aged 21–25 years) participated. None reported any prior tactile disorders. All participants gave informed consent.

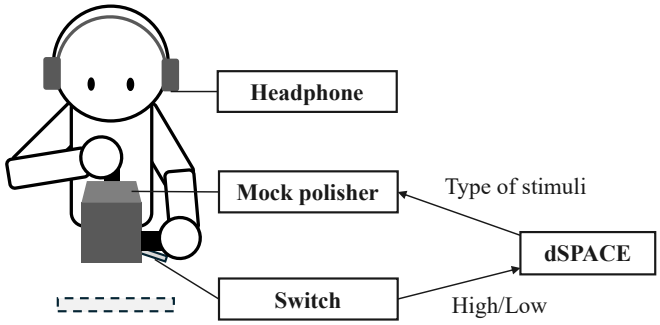

Fig. 7: Schematic representation of the experimental setup. Participants were seated and held the mock polisher. They wore noise-cancelling headphones with white noise and polishing sound to mask out the actuator sound. They pressed the handle switch when they perceived a sign of the mock and to-be polished object contact and press sensation, and released it when they perceived the sign of the mock and the object off.

C. Procedure

Participants were first briefed on the experimental task procedure and shown a video of the professional human polishing behavior recorded under a similar setup and environment reported here. Note that the data obtained in the recording of this video were not included in any of the test trials reported here. They then completed one practice trial.

During each experimental trial, participants held the mock polisher while seated (Fig. 7), experienced one vibration stimulus, and pressed the handle-mounted switch when they perceived contact between the tool and the workpiece. They released the switch when they perceived separation. After each trial, participants completed the subjective evaluation questionnaire. Short rest breaks were provided to minimize fatigue and haptic adaptation. Participants wore noise-cancelling headphone and listened to the white noise and polishing sound at random times to reduce the effect of the sound cues. The Human Ethical Review Committee of Chuo University approved this study (No. 2025-090).

The order of stimulus presentation was counterbalanced at two levels: (i) Across participants, a balanced Latin square ensured that each condition appeared equally often in each ordinal position. (ii) Within each participant, an ABBA sequence was used to mitigate order effects for the two datasets of the same condition.

D. Behavioral Measure: Timing Error

To evaluate the fidelity of transient presentation, we analyzed press and release timing errors. Press timing error was defined as the time difference between the actual contact onset (based on force data) and the participant's press of the switch. Release timing error was defined analogously using the contact offset. One-way ANOVAs were performed separately for press and release errors across the five conditions. If the ANOVA was significant, Tukey–Kramer post-hoc pairwise comparisons were planned a priori, given the anticipated unequal sample sizes across conditions due to non-response trials.

E. Subjective Evaluation

After each trial, participants rated the following statements on a 7-point Likert scale (1 = strongly disagree, 7 = strongly agree):

1) The presented vibration was clear. (*clarity*)
2) The presented vibration felt natural. (*naturalness*)
3) I am confident in the timing of my switch press. (*confidence*)

Following prior findings [21], [22], Likert scores were treated as interval data and analyzed with one-way ANOVA. Tukey's Honest Significant Difference test was applied for post-hoc pairwise comparisons when appropriate.

VI. Results and Discussion

A. Timing Error Analysis

Fig. 8 shows boxplots of press and release timing errors. Press timing error showed no main effect of condition, $F(4, 151) = 0.47$, $p = 0.761$, $\eta_p^2 = 0.012$ (small), and release timing error likewise showed no main effect. While not statistically significant, the comparison between P-LPF and Raw in press timing error showed a small effect size ($d = 0.34$), hinting at a potential benefit of P-LPF.

B. Subjective Evaluation

Fig. 9 shows Likert score distributions for clarity, naturalness, and confidence. The ANOVA results indicated significant main effects of condition for all three subjective measures: clarity, $F(4, 195) = 8.83$, $p < .001$, $\eta_p^2 = 0.153$ (large); naturalness, $F(4, 195) = 2.43$, $p = 0.049$, $\eta_p^2 = 0.0475$ (small); and confidence, $F(4, 195) = 4.15$, $p = 0.003$, $\eta_p^2 = 0.079$ (medium). Post-hoc comparisons (Fig. 10) revealed that Task-Specific Band-Pass achieved significantly higher clarity than all other conditions except Perceptual Low-Pass, which itself scored higher than Original. For naturalness, Task-Specific Band-Pass scored significantly higher than Original. For confidence, Task-Specific Band-Pass outperformed all other conditions.

C. Discussion

Both Press and release timing errors showed no main effect of condition. This suggests that the tested processing strategies did not measurably affect participants' behavioral response accuracy for this simple press/release task. The lack of release timing differences likely stems from the minimal time available to react after stimulus offset, making release actions less sensitive to variations in signal processing. One possible reason for the lack of significant differences is that, in some trials with less perceptible changes, certain participants did not press the switch at all. These missing responses effectively reduced the variability and mean error for those conditions, potentially masking differences that might otherwise have emerged. In our dataset, the number of non-response trials ranged from a maximum of 11 in Raw to a minimum of 7 in TS-BPF, with higher counts generally observed in the less perceptible conditions.

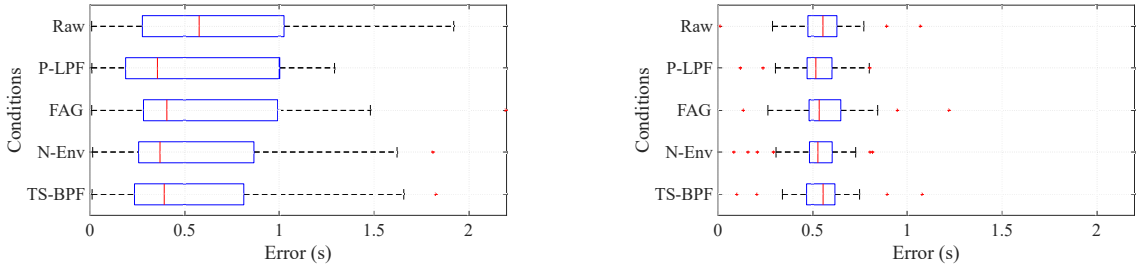

(a) Press (b) Release

Fig. 8: Timing error derived from the reaction time of the switch press and release for each processing condition: (a) press, (b) release. Conditions: Raw = Original, P-LPF = Perceptual Low-Pass, FAG = Frequency-Bin Amplitude Gain, N-Env = Nonlinear Envelope Gain, TS-BPF = Task-Specific Band-Pass. Boxplots show median, interquartile range, and whiskers to 1.5×IQR; outliers are plotted individually.

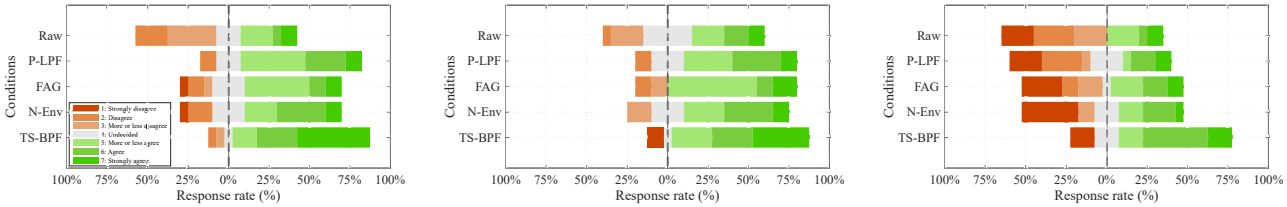

(a) Clarity (b) Naturalness (c) Confidence

Fig. 9: Distribution of Likert scale ratings for each condition: (a) clarity, (b) naturalness, (c) confidence. The horizontal axis represents conditions; the vertical axis represents the percentage of responses. Bars to the right indicate more positive responses. Condition abbreviations are as in Fig. 8.

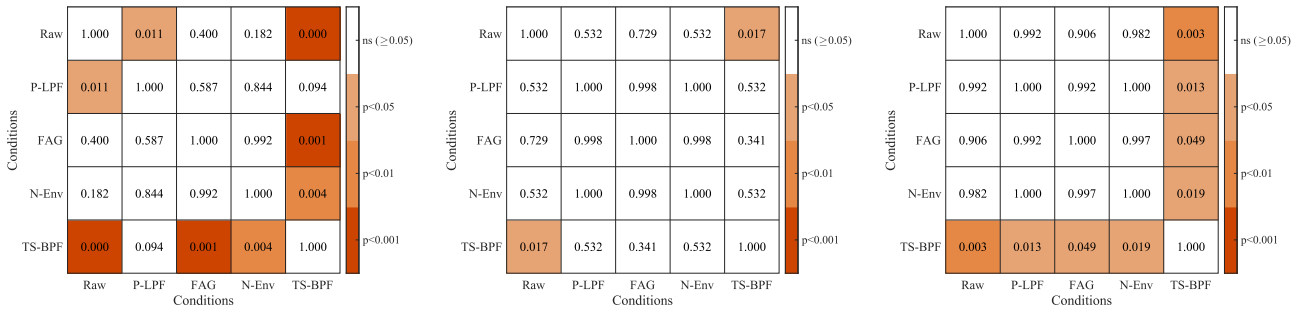

(a) Clarity (b) Naturalness (c) Confidence

Fig. 10: Pairwise comparison p-values (Tukey HSD) for subjective evaluation metrics: (a) clarity, (b) naturalness, (c) confidence. White indicates no significant difference ($p > 0.05$); increasing red saturation indicates stronger significance: light red = $p < 0.05$, medium red = $p < 0.01$, dark red = $p < 0.001$. Condition abbreviations are as in Fig. 8.

In contrast, the subjective evaluation revealed clear advantages for TS-BPF in all three perceptual metrics, with large effect sizes for clarity (η_p^2 = 0.1533) and medium for confidence (η_p^2 = 0.0785). The targeted enhancement of a narrow frequency band characteristic of pressing contact likely made the onset and maintenance of contact more perceptible, thereby increasing participants' confidence in their responses. The improvement in clarity for P-LPF over Raw, which showed a small effect size (η_p^2 = 0.0475), suggests that removing high-frequency content outside the range of human tactile sensitivity can make vibration presentation more distinct, possibly by concentrating actuator output power in perceptually relevant bands.

Overall, these results indicate that while the signal deformation strategies did not significantly alter behavioral timing performance in this task, task-specific spectral emphasis, particularly TS-BPF, can substantially improve subjective perceptual quality, with effect sizes in the large range for clarity and confidence. This aligns with prior findings [23], [24], that perceptual optimization of vibrotactile signals can enhance user experience even in the absence of measurable changes in behavioral task performance.

This study used 10 university students, which limits generalizability. Younger adults often have greater vibro-

tactile sensitivity and lack professional polishing expertise; therefore, effects may be smaller in other populations. With five conditions, n=10 provides limited power to detect small differences. Larger, age- and expertise-diverse samples are needed to confirm robustness.

VII. Conclusion

This study proposed a signal-processing-based approach to improving the perceptual quality of vibrotactile feedback in the teleoperation of skilled manual tasks and experimentally validated its effectiveness using a self-developed mock polisher. Unlike conventional methods that rely on system redesign or complex control strategies, the proposed approach focuses on perceptual modulation of the feedback signal, thus remaining largely hardware-agnostic and a low-cost solution that extends to other tool-mediated tasks once task-specific bands are identified from data.

Perceptual evaluation results indicated that software-based signal processing can enhance vibrotactile feedback quality. In particular, emphasizing perceptually important frequency components identified from task characteristics (TS-BPF) was effective in improving users' subjective experience, especially clarity and confidence, whereas behavioral timing performance remained unaffected.

Future work will integrate the proposed processing into a real-time bilateral control system to examine its effectiveness under dynamic interaction without compromising stability. Extending the evaluation to a variety of polishing tasks will help assess generalizability beyond the simple press/release discrimination used here. Additional directions include investigating applicability to other tool-mediated operations, exploring actuator-specific optimization, and combining perceptual signal enhancement with adaptive control strategies for further improvement of user experience in teleoperation.

References

[1] T. Muender, M. Bonfert, A. V. Reinschluessel, R. Malaka, and T. Döring, "Haptic Fidelity Framework: Defining the Factors of Realistic Haptic Feedback for Virtual Reality," in *CHI Conference on Human Factors in Computing Systems*. New Orleans LA USA: ACM, Apr. 2022, pp. 1–17.

[2] T. Tsuji, Y. Kato, G. Solak, H. Zhang, T. Petrič, F. Nori, and A. Ajoudani, "A Survey on Imitation Learning for Contact-Rich Tasks in Robotics," Jun. 2025.

[3] R. L. Klatzky, D. Pawluk, and A. Peer, "Haptic Perception of Material Properties and Implications for Applications," *Proceedings of the IEEE*, vol. 101, no. 9, pp. 2081–2092, Sep. 2013.

[4] A. Balijepalli and T. Kesavadas, "Value-Addition of Haptics in Operator Training for Complex Machining Tasks," *Journal of Computing and Information Science in Engineering*, vol. 4, no. 2, pp. 91–97, Jun. 2004.

[5] V. Nitsch and B. Färber, "A Meta-Analysis of the Effects of Haptic Interfaces on Task Performance with Teleoperation Systems," *IEEE Transactions on Haptics*, vol. 6, no. 4, pp. 387–398, Oct. 2013.

[6] W. McMahan and K. J. Kuchenbecker, "Spectral Subtraction of Robot Motion Noise for Improved Event Detection in Tactile Acceleration Signals," in *Haptics: Perception, Devices, Mobility, and Communication*, P. Isokoski and J. Springare, Eds. Berlin, Heidelberg: Springer, 2012, pp. 326–337.

[7] K. J. Kuchenbecker, J. Fiene, and G. Niemeyer, "Improving contact realism through event-based haptic feedback," *IEEE Transactions on Visualization and Computer Graphics*, vol. 12, no. 2, pp. 219–230, Mar. 2006.

[8] A. Okamura, M. Cutkosky, and J. Dennerlein, "Reality-based models for vibration feedback in virtual environments," *IEEE/ASME Transactions on Mechatronics*, vol. 6, no. 3, pp. 245–252, Sep. 2001.

[9] X. Wang and P. Liu, "Improvement of haptic feedback fidelity for telesurgical applications," *Electronics Letters*, vol. 42, no. 6, pp. 327–329, Mar. 2006.

[10] H. Ji, S. Li, J. Wang, and Z. Ruan, "Improving Teleoperation Through Human-Aware Haptic Feedback: A Distinguishable and Interpretable Physical Interaction Based on the Contact State," *IEEE Transactions on Human-Machine Systems*, vol. 53, no. 1, pp. 24–34, Feb. 2023.

[11] H.-y. Yao, V. Hayward, and R. E. Ellis, "A tactile enhancement instrument for minimally invasive surgery," *Computer Aided Surgery*, vol. 10, no. 4, pp. 233–239, Jan. 2005.

[12] R. A. MacLachlan, B. C. Becker, J. C. Tabares, G. W. Podnar, L. A. Lobes, and C. N. Riviere, "Micron: An Actively Stabilized Handheld Tool for Microsurgery," *IEEE Transactions on Robotics*, vol. 28, no. 1, pp. 195–212, Feb. 2012.

[13] R. T. Verrillo, A. J. Fraioli, and R. L. Smith, "Sensation magnitude of vibrotactile stimuli," *Perception & Psychophysics*, vol. 6, no. 6, pp. 366–372, Nov. 1969.

[14] P. J. J. Lamoré, H. Muijser, and C. J. Keemink, "Envelope detection of amplitude-modulated high-frequency sinusoidal signals by skin mechanoreceptors." *Journal of the Acoustical Society of America*, vol. 79, no. 4, pp. 1082–1085, Apr. 1986.

[15] N. Cao, H. Nagano, M. Konyo, S. Okamoto, and S. Tadokoro, "Envelope effect study on collision vibration perception through investigating just noticeable difference of time constant," in *2017 IEEE World Haptics Conference (WHC)*, Jun. 2017, pp. 528–533.

[16] H. Nagano, H. Takenouchi, N. Cao, M. Konyo, and S. Tadokoro, "Tactile feedback system of high-frequency vibration signals for supporting delicate teleoperation of construction robots," vol. 34, no. 11, pp. 730–743, Jun. 2020.

[17] R. Hassen and E. Steinbach, "Vibrotactile Signal Compression Based on Sparse Linear Prediction and Human Tactile Sensitivity Function," in *2019 IEEE World Haptics Conference (WHC)*, Jul. 2019, pp. 301–306.

[18] W. Ryuto and T. Toshiaki, "周波数解析を用いてデフォルメした触覚提示 (Haptic presentation deformed using frequency analysis)," 2024.

[19] W. McMahan, J. M. Romano, A. M. Abdul Rahuman, and K. J. Kuchenbecker, "High frequency acceleration feedback significantly increases the realism of haptically rendered textured surfaces," in *2010 IEEE Haptics Symposium*, Mar. 2010, pp. 141–148.

[20] A. Ajoudani, S. B. Godfrey, M. Bianchi, M. G. Catalano, G. Grioli, N. Tsagarakis, and A. Bicchi, "Exploring Teleimpedance and Tactile Feedback for Intuitive Control of the Pisa/IIT SoftHand," *IEEE Transactions on Haptics*, vol. 7, no. 2, pp. 203–215, Apr. 2014.

[21] G. Norman, "Likert scales, levels of measurement and the "laws" of statistics," *Advances in Health Sciences Education*, vol. 15, no. 5, pp. 625–632, Dec. 2010.

[22] C. Mircioiu and J. Atkinson, "A Comparison of Parametric and Non-Parametric Methods Applied to a Likert Scale," *Pharmacy: Journal of Pharmacy, Education and Practice*, vol. 5, no. 2, p. 26, May 2017.

[23] N. Sabnis, A. Otaran, D. Wittchen, J. K. Didion, J. Steimle, and P. Strohmeier, "Foot Pedal Control: The Role of Vibrotactile Feedback in Performance and Perceived Control," in *Proceedings of the Nineteenth International Conference on Tangible, Embedded, and Embodied Interaction*. Bordeaux/Talence France: ACM, Mar. 2025, pp. 1–15.

[24] Y. Gong, H. Mat Husin, E. Erol, V. Ortenzi, and K. J. Kuchenbecker, "AiroTouch: Enhancing telerobotic assembly through naturalistic haptic feedback of tool vibrations," *Frontiers in Robotics and AI*, vol. 11, May 2024.